

Noise2Sim – Similarity-based Self-Learning for Image Denoising

Chuang Niu and Ge Wang
 Rensselaer Polytechnic Institute
 110 8th Street, Troy, New York 12180, USA
 {niu, wanggg6}@rpi.edu

Abstract

The key idea behind denoising methods is to perform a mean/averaging operation, either locally or non-locally. An observation on classic denoising methods is that **non-local mean** (NLM) outcomes are typically superior to locally denoised results. Despite achieving the best performance in image denoising, the supervised deep denoising methods require paired noise-clean data which are often unavailable. To address this challenge, **Noise2Noise** methods are based on the fact that paired noise-clean images can be replaced by paired noise-noise images that are easier to collect. However, in many scenarios collection of paired noise-noise images are still impractical. To bypass labeled images, **Noise2Void** methods predict masked pixels from their surroundings in a single noisy image only. It is pitiful that neither Noise2Noise nor Noise2Void methods utilize self-similarities in an image as NLM methods do, while self-similarities/symmetries play a critical role in modern sciences. Here we propose **Noise2Sim**, an NLM-inspired self-learning method for image denoising. Specifically, Noise2Sim leverages self-similarities of image patches and learns to map between the center pixels of similar patches for self-consistent image denoising. Our statistical analysis shows that Noise2Sim tends to be equivalent to Noise2Noise under mild conditions. To accelerate the process of finding similar image patches, we design an efficient two-step procedure to provide data for Noise2Sim training, which can be iteratively conducted if needed. Extensive experiments demonstrate the superiority of Noise2Sim over Noise2Noise and Noise2Void on common benchmark datasets.

1. Introduction

Image denoising is to recover signals hidden in a noisy background. Since noise is a statistical fluctuation governed by quantum mechanics, denoising is generally achieved by an mean/averaging operation. For example, local averaging methods can perform Gaussian smoothing [17], anisotropic filtering [21][5], and neighborhood filtering [29][24][26].

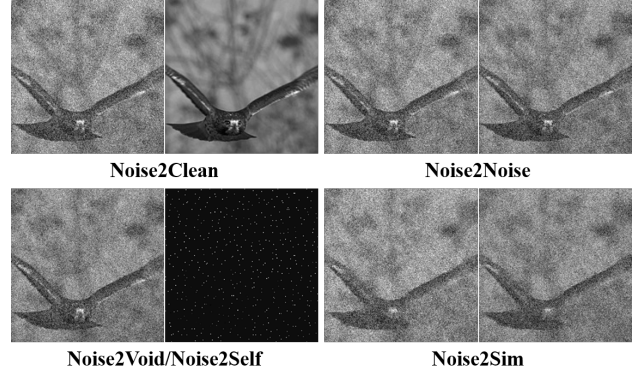


Figure 1. Comparison of training samples for different deep denoising methods. *Noise2Clean* methods require many paired noise-clean samples for network training. *Noise2Noise* method takes paired noise-noise samples in the training process, which are easier to collect than Noise2Clean counterparts but still impractical in many scenarios. Noise2Void and Noise2Self methods propose to predict a small portion of excluded pixels with their local neighbors only using single noisy images during training. Beyond these methods, *Noise2Sim* leverages self-similarities in an image and constructs training images using the single noisy image itself in the same spirit of non-local means, which tends to be equivalent to the Noise2Noise methods.

On the other hand, non-local averaging methods rely on various non-local means with Gaussian kernel based weights [4], or via non-local collaborative filtering in the transform domain [6]. Remarkably, the non-local methods usually outperform the local methods, as images usually consist of self-similar/repeated patterns that can be leveraged in recovering signals coherently. Over recent years, the area of image denoising has been dominated by deep convolutional neural networks (CNNs). Different from the traditional methods that directly denoise an image based on an explicit model, the deep denoising methods optimize a CNN using many training images, and then use the trained model to predict the denoised image, achieving better results at less run time than the traditional non-local methods.

Initially, deep denoising methods require many pairs of

noise-clean images to train the networks. However, such noise-clean image pairs cannot be obtained in many scenarios, preventing these methods from widespread practical applications. To relax the requirement of paired noise-clean samples, the Noise2Noise method [15] trains the CNN with paired noise-noise images that share the same content but instantiated with different noises. It is shown that the Noise2Noise training tends to optimize a network up to a Noise2Clean quality under the assumption of zero-mean independent noises. However, the collection of paired noisy images are not practical either in many scenarios. Therefore, increasingly more efforts are made to develop unsupervised learning methods that train a denoising network with single noisy images. As the first prototype of this kind, the Noise2Void method [12] does not involve paired samples (either Noise2Clean or Noise2Noise data), and yet still predicts the value of each pixel from values of its neighbors. It is pitiful that neither Noise2Noise nor Noise2Void methods utilize self-similarities in an image as NLM methods do, while self-similarities/symmetries play a critical role in modern sciences.

Inspired by the established successes of non-local means [4] and the promising results of Noise2Noise [15], here we propose Noise2Sim to synergize these prior arts. Specifically, our Noise2Sim approach learns a CNN via self-consistent mapping between center pixels of non-local similar patches and enables a new type of unsupervised image denoising possibilities. It is demonstrated for the Noise2Noise method that using paired noisy pixels with zero-mean noise to train a CNN will converge to what the network learns using clean pixels as the target. As paired noise-noise data are often unavailable in real applications, here we propose to bootstrap such paired noisy pixels only from the single noisy images for training a denoising CNN. Under the assumption of non-local methods that an image usually consists of self-similarities/repeated patterns, we globally search for a set of similar patches and co-register them at the central pixels to form an image specific training dataset. Then, these similar central pixels are randomly selected to form new noisy images, which are then paired to train the CNN. In Fig. 1, we compare the training samples for the Noise2Clean, Noise2Noise, Noise2Void/Noise2Self methods, and our Noise2Sim method.

Theoretically, the Noise2Sim method is equivalent to the Noise2Noise method if the values of similar pixels are sufficiently close and noises are independent given specific signals. Ideally, when the difference between the similar pixels is zero, the Noise2Sim result is equivalent to the Noise2Noise counterpart, as explained in Subsection 3.3. Furthermore, a training dataset for Noise2Sim is significantly larger than that for Noise2Void, with the latter being a subset of the former. That is, Noise2Sim is a non-local mean version of Noise2Void. Although it is a non-local

mean method, Noise2Sim is as fast as Noise2Noise and Noise2Void in the inference stage, because it only does the non-local searching for training. And Noise2Sim directly takes an original noisy image as input, and any established denoising CNNs can be adopted without any architectural modification.

Although required in the training stage only, globally searching for similar image patches is a substantial computational burden. On the other hand, the number of similar image patches is very large, as described in Subsection 3.4. If all these patches are pre-computed and sorted before training, the required storage will be overwhelming. To overcome this problem, we design a two-step procedure to select and format similar pixel values efficiently for training a denoising network: *Step 1*: Generate a set of a proper number k of similar images before training, and *Step 2*: Construct the paired noisy images randomly from these similar images on-the-fly during training the network. Also, a refined training strategy can be used for better estimation of similarity between image patches, in hope of further improved denoising results.

The main contributions of this paper are as follows:

- 1) We propose an NLM-inspired self-supervised learning method for image denoising that learns to map between central pixels in similar image patches and only requires single noisy images for training;
- 2) We develop an two-step procedure to manage the computational burden associated with globally searching of similar image patches and prepare training data efficiently for Noise2Sim denoising;
- 3) We design a refined training strategy to use Noise2Sim results for further Noise2Sim denoising, giving improved image quality;
- 4) We perform extensive experiments and statistical analysis, and demonstrate that our Noise2Sim method outperform the state-of-the-art Noise2Void method on common benchmark datasets;
- 5) We make our Noise2Sim software package publicly available.

2. Related Work

Since image denoising has been among the central problems, a large variety of denoising methods were developed over the past decades. Here we briefly review the results most relevant to our proposed Noise2Sim method, especially traditional non-local mean (NLM) methods and deep denoising methods in different supervision modes including fully-supervised, weakly-supervised, and unsupervised or self-supervised learning. It is noted that some of these methods can be used for not only image denoising but also for image restoration (e.g., image super-resolution) and other similar tasks but here we only focus on image denoising.

2.1. Non-local Mean Methods

Non-local means (NLM) [4] is a classic non-local denoising approach. In contrast to the local denoising methods that use a mean value of a group of pixels surrounding a target pixel for its refinement, NLM takes a weighted mean of all pixels in an image, where the weights are determined by similarities of the image patches where these pixels are centrally located to the image patch for the target pixel. Often times, NLM reveals more details with better clarity than local denoising methods. The basic idea of non-local methods is that most images contain self-similarities/repeated patterns that can be utilized to augment data and recover signals. Based on this idea, many non-local methods were developed, such as BM3D [6], LSSC [19], NCSR [7], and WNNM [8], just to name a few. Despite their superior performance, the non-local mean methods demand longer searching time, which is a practical issue in many applications such as real-time video image processing.

2.2. Deep Denoising Methods

Fully-supervised deep denoising methods train a CNN with many paired noise-clean images that can be curated in advance. Jain *et al.* first formulated denoising as a regression task and trained a CNN by minimizing a loss function of the prediction and clean targets [10], which is a standard framework for deep image denoising. In [30], a very deep CNN architecture for residual learning was introduced, effectively handling multiple levels of noise. At the same time, in [20] a very deep encoding-decoding model was designed with skip-layer connections for image restoration. In [25], a very deep persistent memory network was used with a memory block also for image restoration. In the context of fluorescence microscopy, a content-aware image restoration method was introduced along with freely available software [27]. Although the supervised denoising/restoration methods were successfully applied to a variety of problems, they critically depend on paired noise-clean data which are costly to prepare or impractical to collect.

Weakly-supervised deep denoising method relax the requirement of paired noise-clean images to the use of paired noise-noise data or unpaired noise and clean images. The Noise2Noise method [15] uses paired noisy images to train a CNN to achieve an equivalent denoising performance under the assumption of zero-mean noise. In [28], Wu *et al.* proposed a two-step unpaired learning method for image denoising. They first leverage the self-learning methods to train a denoising model and a noising model, which are then applied on the unpaired noisy and clean images respectively to generate paired datasets. Finally, the generated datasets are used to train the final denoising model in the supervised learning manner.

Unsupervised deep denoising methods have recently attracted a major attention because they are least restrictive

and most desirable in practice, where only single noisy images are available and need to be denoised. The Noise2Void method [12] and the concurrent Noise2Self method [2] train a network to predict masked pixels using their neighbors. Interestingly, in [13] a Probabilistic Noise2Void model users a maximum likelihood strategy to predict per-pixel intensity distributions instead of a specific pixel value only. Based on Noise2Void, Laine *et al.* redesigned the blind-spot network that takes several rotated input images as the input and merge the corresponding outputs though a series of 1×1 convolutions [14]. Then, assuming a known noise distribution a Bayesian reasoning strategy was proposed to optimize this blind point network. In [3], a Structured Noise2Void method was presented to remove structured noise by modifying the blind mask, assuming a known noise configuration. Of particular interest, several deep denoising methods focus on training and testing on a single noisy image. The deep image prior method [16] trains a CNN to predict a noisy image of interest from a random but uniform noise, and obtain a denoised image when this process is properly terminated before convergence. In this case, the training process is also the inference process. Recently, Quan *et al.* suggested a Self2Self method that trains a network by mapping between random dropout images obtained with an independent Bernoulli sampling from a single noisy image [22]. In the testing stage, the trained network takes a set of independent Bernoulli sampled dropout images as the input, and averages all predictions as the output. Note that the networks of this type need to be trained for each image, and may not deliver a real-time performance.

3. Method

While Noise2Noise, Noise2Void and Noise2Self methods generate promising results, they miss opportunities of utilizing self-similar features in an image on which NLM methods capitalize to outperform classic local denoising methods. Synergizing Noise2Noise and well-established NLM ideas, here we propose **Noise2Sim** as a novel self-supervised learning method that is trained off-line on a set of images and deployed in real-time applications.

3.1. Assumptions

First, let us analyze the assumptions of deep denoising methods in different supervision modes, and introduce the assumptions for the proposed Noise2Sim method. To reduce or avoid the burden of collecting paired noise-clean data, weakly-supervised and unsupervised learning methods depend on additional assumptions. Typically, a noisy image $\mathbf{x} = \mathbf{s} + \mathbf{n}$ is drawn from a joint distribution in the form of $p(\mathbf{s}, \mathbf{n}) = p(\mathbf{s})p(\mathbf{n}|\mathbf{s})$.

Fully-supervised deep denoising methods do not depend on additional assumptions as long as paired noise-clean data can be obtained. With paired noise-noise data, Noise2Noise

relies on the assumption that the noise has a zero mean, i.e., $\mathbb{E}[n_i] = 0$, which leads to $\mathbb{E}[x_i] = s_i$, where i denotes the pixel index. Since learning to map between paired noisy pixels forces the network outputting the mean value [15], the zero-mean noise assumption ensures that the predicted values are the true signals.

The unsupervised Noise2Void method requires single noisy images for training and more assumptions as follows:

- Zero-mean noise, the same as for Noise2Noise;
- Conditional independence of noise given the signal values, i.e., $p(\mathbf{n}|\mathbf{s}) = \prod_i p(n_i|s_i)$;
- Local predictability, meaning that two pixels i and j (within a certain distance) are not independent, i.e., $p(s_i|s_j) \neq p(s_i)$.

The local predictability explains why the center pixel can be predicted by data from its neighborhood, and why the blind-spot network for Noise2Void works. The conditional independence indicates that the noise is not predictable so that the predicted noises will converge to zero, under the zero-mean assumption. Therefore, the signal is predicted while the noise is removed.

Our proposed Noise2Sim method performs unsupervised learning, and shares the first two assumptions for Noise2Void, and requires:

- Existence of non-local similar image patches, which means that for a reference pixel there exists a set of similar pixels defined as the corresponding image patches respectively centralized at these pixels are similar by a certain measure.

The existence of non-local similar pixels reflects similarity, periodicity, symmetry, and sparsity commonly observed in practice and successfully utilized in traditional non-local mean denoising tasks. As shown in Figure 2, images usually contain repeated features so that a group of similar pixels can be obtained for noise cancellation. Our Noise2Sim method finds similar image patches to synthesize image pairs and train a denoising model, in a sharp contrast to the Noise2Void and Noise2Self methods that ignore such inherent informational structures.

3.2. Noise2Sim

For Noise2Sim denoising, paired training samples are first found from a single noisy image since traditionally paired noise-clean or noise-noise data are unavailable. To better understand Noise2Sim, we first describe Noise2Clean, Noise2Noise, and Noise2void mappings. In terms of the receptive field of a selected denoising CNN, each pixel y_i in its output image is predicted by a corresponding patch $X_{RF(i)}$ specified by x_i as the center pixel;

that is, $y_i = f(X_{RF(i)}, \theta)$, where f denotes a network function with the vector of parameters θ to be optimized.

During training, a loss function is minimized as follows:

$$\arg \min_{\theta} \sum_{n=1}^N \sum_{i=1}^{HW} L(f(X_{RF(i)}^n), y_i^n), \quad (1)$$

where the loss function L can be the mean squared error (MSE), N is the number of images, H and W are the height and width of an image respectively, and y_i^n is a scalar for a grey-scale image and a vector for a spectral image. The difference among Noise2Clean, Noise2Noise and Noise2Void methods lies in the training samples $\{X_{RF(i)}^n, y_i^n\}$. In the Noise2Clean case, $X_{RF(i)}^n$ is an input image patch with pixel x_i at the center, and $y_i^n = s_i^n$ is the clean target. In the Noise2Noise case, the target $y_i^n = x_i'^n$ is from the paired noisy image, while the input remains the same as that for Noise2clean. As far as Noise2Void is concerned, each image patch in an input noisy image has its central pixel x_i masked, i.e., $X_{RF(i)}^n / \{x_i^n\}$, and the target $y_i^n = x_i^n$ is the central pixel x_i , which is blocked in the input image patch.

Different from the above cases, to construct training samples for Noise2Sim, we first search for a set of k similar pixels, denoted as $\mathcal{S}_k(x_i^n)$, for each pixel x_i^n in a noisy image. The similarity between two pixels is measured with the Euclidean distance between the two image patches whose centers are the two pixels respectively (in this study, we assume that each patch covers a square region). In Fig. 2, a number of similar patches are shown over an input noisy image, where the green boxes denote the patches most similar to the input patch containing the yellow pixel. Correspondingly, the central pixels of these patches are defined as similar pixels with respect to the reference pixel x_i^n . Let us denote training samples for Noise2Sim as $\{\widehat{X}_{RF(i)}^n, \widehat{x}_i^n\}$, where the target pixel \widehat{x}_i^n is randomly selected from $\mathcal{S}_k(x_i^n) \cup x_i^n$, and each pixel in $\widehat{X}_{RF(i)}^n$ is also randomly and independently selected from its corresponding set of similar $k+1$ pixels (+1 means the reference pixel included). Therefore, the set of training samples for Noise2Sim is much larger than that for Noise2Void.

3.3. Statistical Analysis

As introduced in [15], the paired noise pixels $\{x_i, x_i'\}$ are

$$x_i = s_i + n_i, x_i' = s_i + n_i'. \quad (2)$$

where n_i' and n_i are noises. Learning to map between such paired noisy pixels with the MSE loss, the network parameters will be optimized to output the expectation of the noisy targets, i.e., $\mathbb{E}(x_i')$. With the zero mean noise, the output of the optimized network approximates $\mathbb{E}(x_i') = s_i$. That is, the noisy pixel targets are equivalent to the clean signal targets. More specifically, given a finite number of data, the

expected squared difference between mean values of noisy data and the true signals is (see [15] and the supplementary material for details):

$$\mathbb{E}_{\hat{x}} \left[\frac{1}{M} \sum_p s_p - \frac{1}{M} \sum_p x'_p \right]^2 = \frac{1}{M^2} \text{Var}(\sum_p x'_p) \quad (3)$$

That is, the variance of the estimate is the variance of the sum of noisy pixel values, normalized by the squared number of samples M^2 . The error approaches zero with increasing the number of samples so that the noise targets tend to be equivalent to the clean targets.

Similarly, we can compute the difference between the noisy similar pixels and the ideal pixels. In this case, each noisy similar pixel can be decomposed as follows:

$$\hat{x}_i = \hat{s}_i + n_i = s_i + \delta_i + n_i, \quad (4)$$

and with the zero-mean noise assumption we have

$$\mathbb{E}(\hat{x}) = \mathbb{E}(\hat{s}_i) = \mathbb{E}(s_i) + \mathbb{E}(\delta_i), \quad (5)$$

where \hat{s}_i denotes a similar pixel of the true signal s_i , and δ_i denotes the difference between s_i and \hat{s}_i . Then, the expected squared difference between the mean values of similar and true pixels is (see the supplementary material for details):

$$\mathbb{E}_{\hat{x}} \left[\frac{1}{\widehat{M}} \sum_p (s_p - \hat{x}_p) \right]^2 = \frac{1}{\widehat{M}^2} \text{Var}(\sum_p x_p) + \left(\frac{1}{\widehat{M}} \sum_p \delta_p \right)^2. \quad (6)$$

where \widehat{M} is the number of similar pixels. Compared with Eq. (3), Eq. (6) has an additional error term that is the difference between similar and clean pixels. Ideally, if we can find a perfect set of similar pixels for every reference pixel, i.e., $\forall p, \delta_p = 0$, then Eq. (6) is the same as Eq. (3) so that Noise2Sim is equivalent to Noise2Noise (see Subsection 4.5). Although it is impossible to obtain a set of such perfect pixels in practice, the true signals of k -nearest similar pixels are often very closed to each other, as shown in our results below. In addition, the number of similar samples \widehat{M} is significantly larger than that of noisy samples M as described in Subsection 3.4, reducing the first error term in Eq. (6). Therefore, Noise2Sim training with noisy similar pixels tends to be comparable to or even better than Noise2Noise training with paired noisy pixels.

3.4. Noise2Sim training

Although Noise2Sim is statistically sound under the aforementioned assumptions, how to efficiently construct training samples is not trivial. It is well known that globally searching for similar pixels has a large computational cost. Specifically, the similarity of two patches associated with central pixels x_i and x_j is computed as $\|v(\mathcal{N}_i) - v(\mathcal{N}_j)\|_2$,

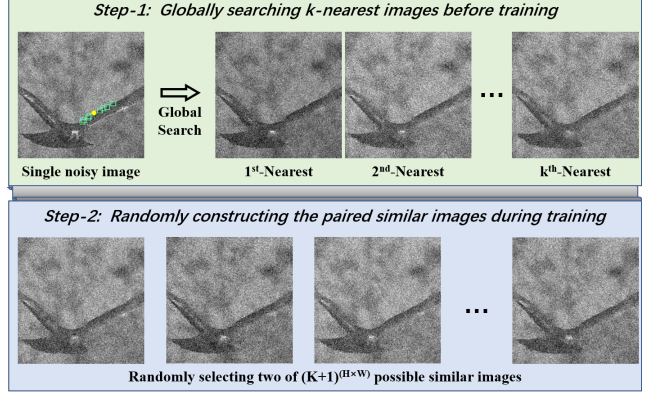


Figure 2. Process of generating data for Noise2Sim training. Step 1 is to find a set of k similar pixels for each reference pixel in a single noisy image, and form k similar images by pixel-wise randomly picking up k corresponding similar pixels. In the exemplary noisy image, the yellow point denotes the reference pixel, and the green boxes present its k -nearest patches whose central pixels are defined as similar pixels. Step 2 is to construct paired images from the $(k + 1)$ similar images obtained in Step 1.

where $\|\cdot\|_2$ denotes the Euclidean distance, $v(\mathcal{N}_p)$ is the vector of pixel values, and \mathcal{N}_p denotes a square patch of an appropriate size and centered at a pixel x_p . For a pixel in a noisy image, we need to globally search for its k -nearest similar patches, from which two central pixels are randomly selected as the input and target pixels respectively. To construct a pair of similar images for Noise2Sim training, the above process are independently repeated pixel by pixel. Clearly, the number of all possible similar images is $(k + 1)^{H \times W}$. If all pairs of similar images are prepared before training or searching on-the-fly during training, the memory space or computational time will be unacceptable.

To overcome above problem, we propose to divide the Noise2Sim training process into two steps. First, we generate k -nearest similar images from a single noisy image, which is a preprocessing step. The k -nearest similar images are obtained by sorting the k -nearest similar pixels for each and every pixel location, as shown in Fig. 2. Given the $k + 1$ similar images (+1 means the original noisy image inclusive), then, we randomly and independently construct a pair of similar images in pixel-wise on-the-fly during training. The two-step training strategy allows a real-time construction of paired similar images at little cost, and the searching time of these similar images is also acceptable using an advanced searching algorithm implemented on GPU. Certainly, there are alternative ways to select the training pairs; see our comparative study in Subsection 4.3.1. After training, the network takes the original noisy image and produces an denoised image. Since noises may harm the estimation of signal similarities, we propose to use the denoised image to further compute the similarity between signals and

conduct Noise2Sim training again, which can be iteratively conducted if necessary.

4. Experiments

4.1. Implementation Details

For a fair comparison, the two-layer UNet [23] with the batch normalization [9] and residual learning was used through all our experiments, which is exactly the same as the network used for Noise2Void. Although the denoising performance can be improved with more advanced architectures, here we focus on demonstrating the feasibility and power of our novel NLM-inspired self-learning method for unsupervised denoising, instead of optimizing any particular architecture. For fast computation of similarity between image patches, we used a publicly available library¹, which is powered by GPU. In the training stage, we used the same augmentation strategy used for Noise2Void, including random cropping followed by random 90°-rotation and mirroring. The Adam [11] algorithm with the cosine learning rate schedule [18] was deployed for training, with the initial learning rate 0.0005. Our method was implemented on the PyTorch² deep learning platform.

4.2. Datasets

We evaluated our proposed Noise2Sim and competitive methods on both simulated and real datasets, including commonly used BSD68 and BSD400 [30] that consist of gray-scale images, BSD500 [1] and Kodak³ containing color images, and the fluorescence microscopy datasets Fluo-C2DL-MSD (MSD) and Fluo-N2DH-GOWT1 (GOWT1) only containing noisy images from the Cell Tracking Challenge. We also constructed a set of piece-wise constant phantom images added with Gaussian noises for assessing the denoising performance of Noise2Sim under the ideal condition and added with structured noises for evaluating the possibility of extending Noise2Sim to process the structured noises (see the supplementary material for details). We used the peak signal-to-noise ratio (PSNR) to quantify the denoising performance.

4.3. Ablation Study

We evaluated alternative methods of pairing similar pixels for training the network, analyzed the hyperparameters that affect the selection of similar pixels, and tested the effectiveness of the iterative training strategy. For these purposes, we used the BSD400 dataset consisting of 400 180 × 180 gray images for training, and the BSD68 dataset containing 68 gray images for testing. Gaussian noise with zero mean and different standard deviations were added.

¹<https://github.com/facebookresearch/faiss>

²<https://pytorch.org/>

³<http://r0k.us/graphics/kodak/>

Table 1. Results with different methods for pairing similar pixels in patches of 3×3 for $k = 8$ and Gaussian noise Std 25.

Pairing Method	1	2	3	4
PSNR	27.12	27.78	27.48	28.15

Table 2. Effects on PSNR of image patch sizes vs. Gaussian noise levels.

S \ Std	5	15	25	35	45	55	65	75
3×3	33.85	29.90	28.14	26.73	25.73	24.89	24.06	23.45
5×5	34.32	29.98	28.02	26.72	25.69	24.93	24.03	23.45
7×7	33.13	29.87	27.93	26.70	25.67	24.83	24.02	23.74
11×11	32.10	29.82	27.43	26.56	25.69	24.86	24.25	23.71
15×15	31.97	28.96	27.58	26.53	25.67	24.94	24.18	23.68

4.3.1 Pairing Methods

Given a set of $k + 1$ similar images as described in Subsection 3.4, there are four reasonable methods for pairing them: 1) Pair the original noisy image as the input to its randomly constructed similar image as the target; 2) reverse the input and label used in 1); 3) pair the two of k sorted similar images without pixel-wise randomization; and 4) pair similar images that were randomly and independently constructed in a pixel-wise. The results in Table 1 demonstrate that the fourth method achieves the best denoising performance. An explanation to this finding is that the fourth method represents diverse samples most effectively without any significant bias.

4.3.2 Hyper-parameters

In the proposed Noise2Sim method, searching for an appropriate set of similar pixels for each reference pixel is a core task. In the search process, a size-fixed square patch window is translated over a noisy image of interest to find similar pixels. Hence, the patch size, denoted by S , is a key parameter that affects the accuracy of similarity measurement. The effect of different patch sizes vs. different Gaussian noise levels on PSNR are shown in Table 2. It can be seen in general that the denoising performance of smaller patch sizes is better for lower noise levels but that of larger patch sizes is better for higher noise levels. This is due to the fact that it requires more contextual information to estimate the similarity accurately when pixels are heavily corrupted by noise.

Moreover, the number of selected similar pixels k determines the error term δ defined in Subsection 3.3. Then, we evaluated the effects of different numbers of selected similar pixels on the denoising performance as shown in Table 3. The results show that the best denoising performance was generally associated with $k = 8$ in our comparative study. These results are attributed to the fact that there is a trade-off between the error term and the number of train-

Table 3. Effects on PSNR of different numbers of similar pixels vs. different patch sizes for $k = 8$ and Gaussian noise Std 25.

$S \backslash k$	2	4	8	16	32	64
3×3	26.93	27.90	28.15	28.08	27.95	27.01
5×5	26.95	27.84	28.02	26.24	26.55	25.94
7×7	26.91	27.68	27.93	27.71	27.50	27.28
11×11	26.81	27.58	27.43	27.23	25.21	25.02
15×15	26.78	27.15	27.58	26.57	26.47	24.76

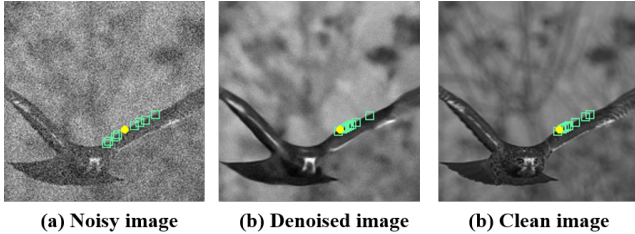


Figure 3. Distribution of similar patches in (a) an original noisy image, (b) the denoised image, and (c) the clean image.

Table 4. Results of Noise2Sim with and without iterative training with respect to different Gaussian levels.

Std	5	15	25	35	45	55	65
<i>W/O</i>	33.85	29.90	28.14	26.73	25.73	24.89	24.06
<i>With</i>	34.15	30.25	28.27	26.98	25.75	24.88	24.02
<i>Upper</i>	34.22	30.54	28.60	27.14	26.08	25.15	24.33

ing samples. Specifically, increasing the number of similar pixels will increase δ values, while decreasing this number will decrease the amount of information on self-similarity. It seems that a decent balance is $k = 8$ in our experiments.

4.3.3 Iterative Training

Any estimate of similarity between image patches is necessarily compromised in a noisy image, such an estimate can be improved in a denoised image produced by a trained denoising model. That is, the Noise2Sim idea can be repeatedly applied to refine the resultant denoising model iteratively. By doing so, the similarity measures will be likely improved, leading to a superior denoising performance. Fig. 3 shows the change in the distribution of similar image patches after one iteration, and the distribution in the denoised image is very close to that in the clean image. We also computed the upper limit for the iterative training by computing the similarity measures using the clean image. Table 4 shows that the iterative training enhances the denoising performance, especially when images are not severely corrupted.

4.4. Comparative Denoising Results

In this Subsection, we compared our Noise2Sim method with the Noise2Clean, Noise2Noise, Noise2Void, and NLM

Table 5. Comparison of denoising results using different methods on different datasets.

Dataset	N2C	N2N	N2V	NLM	Noise2Sim
BSD68-G25	28.96	28.89	27.72	27.58	28.27
BSD68-P30	28.08	28.01	27.08	24.65	27.42
Koak-G25	32.45	32.08	31.02	29.38	31.34
Koak-P30	31.74	31.53	30.45	25.99	30.54

Table 6. Result using different denoising methods on the datasets corrupted by Gaussian noise at different levels.

Std	5	15	25	35	45	55	65	75
<i>N2C</i>	37.89	31.62	28.14	27.33	26.17	25.33	24.58	24.05
<i>N2N</i>	37.84	31.39	28.02	26.15	24.71	23.50	22.59	21.64
<i>N2V</i>	31.81	29.26	27.72	26.61	25.36	24.84	23.95	23.50
<i>NLM</i>	35.31	29.92	27.58	26.07	24.95	24.06	23.29	22.63
<i>N2S</i>	34.15	30.25	28.27	26.98	25.75	24.89	24.06	23.45

methods on the same datasets and using the same network architecture. The PSNR results are shown in Table 5, which indicates that Noise2Sim is better than the NLM and Noise2Void methods. The results are visualized in Fig. 4, showing that our Noise2Sim method can effectively remove Gaussian and Poisson noises in grayscale and color images, especially in real application images. The PSNR values of individual images also indicate that Noise2Sim can achieve better results than Noise2Void and NLM. As the images in MSC and GOWT1 do not have the corresponding ground truth or co-registered independent noisy duplicate, the Noise2Clean and Noise2Noise methods cannot be applied. In [15], the authors pointed out a limitation of the Noise2Void method that it cannot preserve grainy features when the local predictability is in question. Consistent to the known limitation, some grainy structures are missed in our verified Noise2Void images, with some black "holes" presented, as shown in the zoom-in regions of the last two rows in Fig. 4. In contrast, our Noise2Sim images well preserve structural subtleties, as information on self-similarities is fully utilized in our training stages.

4.5. Results on Simulated Ideal Dataset

This study evaluated the denoising performance of the Noise2Sim method under the ideal condition that $\delta = 0$, which is denoted as *Noise2Sim-GT*. To satisfy this condition, we construed a set of piece-wise constant phantom images corrupted by Gaussian noise with *Std* 25. When constructing the training samples for *Noise2Sim-GT*, we assumed the known masks over the piece-wise regions, and thus k pixels in the same region of the reference pixel were randomly selected as its k -nearest similar pixels. The rest steps remained the same as those described in Subsection 3.4. The results using different denoising methods on the simulated dataset are in Fig. 5, demonstrating the Noise2Sim-GT method is indeed equivalent to the

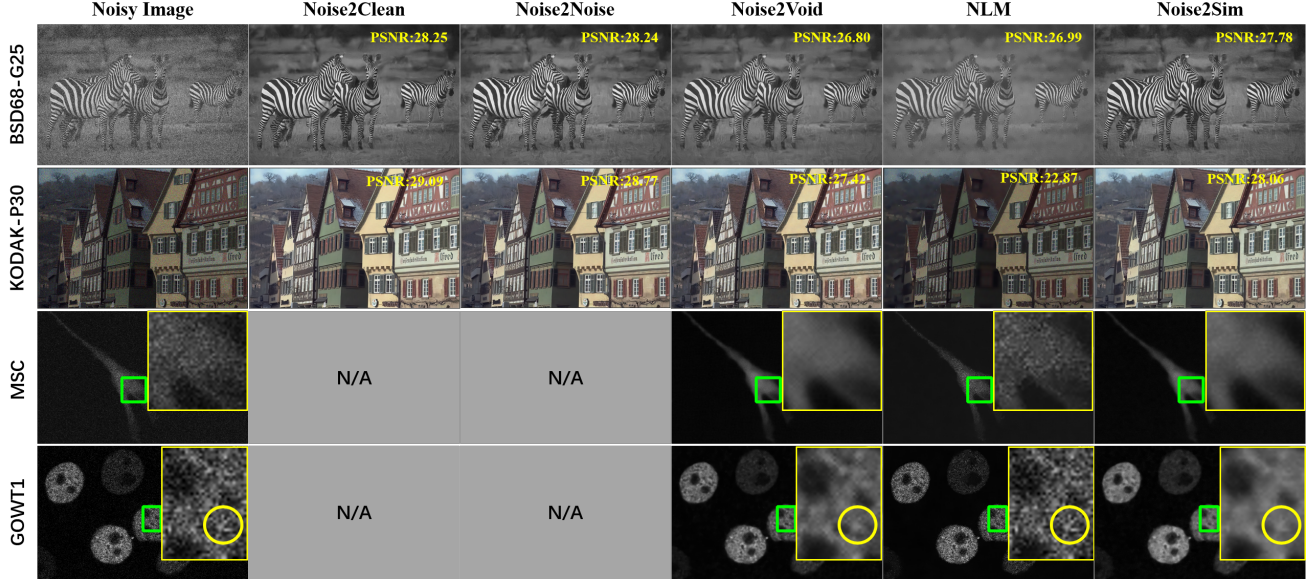


Figure 4. Visual comparison of denoising results on different datasets, where *G2* means Gaussian noise with $Std = 25$, and *P30* means Poisson noise with $\lambda = 30$. For the images with the ground truth, their PSNR values are included. For the GOWT1 and MSC datasets only contain noisy images so that the results of *Noise2Clean* and *Noise2Noise* are not available. The yellow boxes show the zoom-in regions, and the yellow circles emphasize structural details for visual inspection (Refer to the supplementary material for more results).

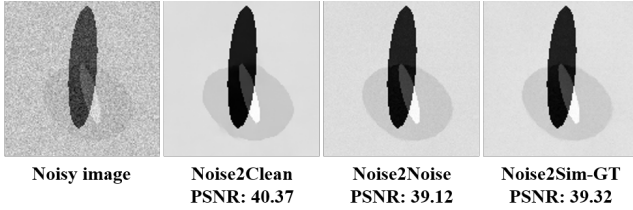


Figure 5. Result obtained using different denoising methods on the simulated dataset, with the PSNR values on the test dataset.

Noise2Noise method and being consistent to the analysis in Subsection 3.3.

5. Discussions

The conditional independence assumption does not support the use of Noise2Sim in suppressing structural noise, which is also the limitation of Noise2Void. Recently, an variant of Noise2Void, Structured Noise2Void [3], was proposed to remove horizontally or vertically correlated noise. Along this and other directions, we can extend Noise2Sim for more types of noises. Specifically, with segmentation masks available, similar patches can be more likely found in similar regions and better paired to generate data for network training. Also, pixel-level mappings can be generalized to patch-level mappings so that coherent noises can be better suppressed. Although we mainly focus on that Noise2Sim is trained on a set of noisy images and then tested on another noisy image in the same domain, its ef-

fectiveness for training and testing on a single noisy image is also evaluated. More experimental results can be found in the supplementary material.

It is underlined that in this initial study the Euclidean distance is used to measure the similarity between patches. More advanced measures can be used for the same purpose at an increased computational cost. Self-similarity exhibits itself in many ways: direct as measured by the Euclidean distance, indirect through scaling, reflection and rotation, or even hidden in a transform domain. Hence, Noise2Sim can be further developed for an optimized performance in a task-specific fashion.

6. Conclusion

We have presented a novel similarity-oriented self-learning approach for image denoising that only requires single noisy images to train the CNN. Theoretically, we have compared the Noise2Clean, Noise2Noise, and Noise2Sim methods, and shown that they tend to be equivalent under mild practical conditions. Technically, a two-step learning scheme has been designed for efficient training data generation. The experimental results have systematically demonstrated the feasibility and superiority of Noise2Sim on both simulated and real datasets. Furthermore, our Noise2Sim approach can be extended from multiple views, such as using finer similarity measures between pixels/patches, extracting more self-similarity information, incorporating the Bayesian reasoning, and removing correlated noises in specific applications.

References

- [1] Pablo Arbelaez, Michael Maire, Charless Fowlkes, and Jitendra Malik. Contour detection and hierarchical image segmentation. *IEEE Trans. Pattern Anal. Mach. Intell.*, 33(5):898–916, May 2011. 6
- [2] Joshua Batson and Loic Royer. Noise2Self: Blind denoising by self-supervision. volume 97 of *Proceedings of Machine Learning Research*, pages 524–533. PMLR, 09–15 Jun 2019. 3
- [3] C. Broaddus, A. Krull, M. Weigert, U. Schmidt, and G. Myers. Removing structured noise with self-supervised blind-spot networks. In *2020 IEEE 17th International Symposium on Biomedical Imaging (ISBI)*, pages 159–163, 2020. 3, 8
- [4] A. Buades, B. Coll, and J. . Morel. A non-local algorithm for image denoising. In *2005 IEEE Computer Society Conference on Computer Vision and Pattern Recognition (CVPR’05)*, volume 2, pages 60–65 vol. 2, 2005. 1, 2, 3
- [5] Francine Catté, Pierre-Louis Lions, Jean-Michel Morel, and Toméu Coll. Image selective smoothing and edge detection by nonlinear diffusion. *SIAM Journal on Numerical Analysis*, 29(1):182–193, 1992. 1
- [6] K. Dabov, A. Foi, V. Katkovnik, and K. Egiazarian. Image denoising by sparse 3-d transform-domain collaborative filtering. *IEEE Transactions on Image Processing*, 16(8):2080–2095, 2007. 1, 3
- [7] W. Dong, L. Zhang, G. Shi, and X. Li. Nonlocally centralized sparse representation for image restoration. *IEEE Transactions on Image Processing*, 22(4):1620–1630, 2013. 3
- [8] S. Gu, L. Zhang, W. Zuo, and X. Feng. Weighted nuclear norm minimization with application to image denoising. In *2014 IEEE Conference on Computer Vision and Pattern Recognition*, pages 2862–2869, 2014. 3
- [9] Sergey Ioffe and Christian Szegedy. Batch normalization: Accelerating deep network training by reducing internal covariate shift. volume 37 of *Proceedings of Machine Learning Research*, pages 448–456, Lille, France, 07–09 Jul 2015. PMLR. 6
- [10] Viren Jain and Sebastian Seung. Natural image denoising with convolutional networks. In D. Koller, D. Schuurmans, Y. Bengio, and L. Bottou, editors, *Advances in Neural Information Processing Systems 21*, pages 769–776. 2009. 3
- [11] Diederik P. Kingma and Jimmy Ba. Adam: A method for stochastic optimization. In Yoshua Bengio and Yann LeCun, editors, *ICLR*, 2015. 6
- [12] A. Krull, T. Buchholz, and F. Jug. Noise2void - learning denoising from single noisy images. In *2019 IEEE/CVF Conference on Computer Vision and Pattern Recognition (CVPR)*, pages 2124–2132, 2019. 2, 3
- [13] Alexander Krull, Tomáš Vičar, Mangal Prakash, Manan Lalit, and Florian Jug. Probabilistic noise2void: Unsupervised content-aware denoising. *Frontiers in Computer Science*, 2:5, 2020. 3
- [14] Samuli Laine, Tero Karras, Jaakko Lehtinen, and Timo Aila. High-quality self-supervised deep image denoising. In H. Wallach, H. Larochelle, A. Beygelzimer, F. Alche-Buc, E. Fox, and R. Garnett, editors, *Advances in Neural Information Processing Systems 32*, pages 6970–6980. 2019. 3
- [15] Jaakko Lehtinen, Jacob Munkberg, Jon Hasselgren, Samuli Laine, Tero Karras, Miika Aittala, and Timo Aila. Noise2Noise: Learning image restoration without clean data. volume 80, pages 2965–2974, 10–15 Jul 2018. 2, 3, 4, 5, 7
- [16] V. Lempitsky, A. Vedaldi, and D. Ulyanov. Deep image prior. In *2018 IEEE/CVF Conference on Computer Vision and Pattern Recognition*, pages 9446–9454, 2018. 3
- [17] M Lindenbaum, M Fischer, and A Bruckstein. On gabor’s contribution to image enhancement. *Pattern Recognition*, 27(1):1 – 8, 1994. 1
- [18] I. Loshchilov and F. Hutter. Sgdr: Stochastic gradient descent with warm restarts. In *ICLR*, 2017. 6
- [19] J. Mairal, F. Bach, J. Ponce, G. Sapiro, and A. Zisserman. Non-local sparse models for image restoration. In *2009 IEEE 12th International Conference on Computer Vision*, pages 2272–2279, 2009. 3
- [20] Xiaojiao Mao, Chunhua Shen, and Yu-Bin Yang. Image restoration using very deep convolutional encoder-decoder networks with symmetric skip connections. In D. D. Lee, M. Sugiyama, U. V. Luxburg, I. Guyon, and R. Garnett, editors, *Advances in Neural Information Processing Systems 29*, pages 2802–2810. 2016. 3
- [21] P. Perona and J. Malik. Scale-space and edge detection using anisotropic diffusion. *IEEE Transactions on Pattern Analysis and Machine Intelligence*, 12(7):629–639, 1990. 1
- [22] Yuhui Quan, Mingqin Chen, Tongyao Pang, and Hui Ji. Self2self with dropout: Learning self-supervised denoising from single image. In *Proceedings of the IEEE/CVF Conference on Computer Vision and Pattern Recognition (CVPR)*, June 2020. 3
- [23] Olaf Ronneberger, Philipp Fischer, and Thomas Brox. U-net: Convolutional networks for biomedical image segmentation. In Nassir Navab, Joachim Hornegger, William M. Wells, and Alejandro F. Frangi, editors, *MICCAI*, pages 234–241, 2015. 6
- [24] S M Smith and J M Brady. SUSAN-A New Approach to Low Level Image Processing. *Int. Journal of Computer Vision*, 23(1):45–78, 1997. 1
- [25] Ying Tai, Jian Yang, Xiaoming Liu, and Chunyan Xu. Memnet: A persistent memory network for image restoration. In *Proceedings of the IEEE International Conference on Computer Vision (ICCV)*, Oct 2017. 3
- [26] C. Tomasi and R. Manduchi. Bilateral filtering for gray and color images. In *Sixth International Conference on Computer Vision (IEEE Cat. No.98CH36271)*, pages 839–846, 1998. 1
- [27] Martin Weigert, Uwe Schmidt, Tobias Bothe, Andreas Müller, Alexandr Dibrov, Akanksha Jain, Benjamin Wilhelm, Deborah Schmidt, Coleman Broaddus, Siân Culley, Mauricio Rocha-Martins, Fabián Segovia-Miranda, Caren Norden, Ricardo Henriques, Marino Zerial, Michele Solimena, Jochen Rink, Pavel Tomancak, Loic Royer, Florian Jug, and Eugene W. Myers. Content-aware image restoration: Pushing the limits of fluorescence microscopy. *Nature Methods*, 15(12):1090–1097, 2018. 3
- [28] Xiaohe Wu, Ming Liu, Yue Cao, Dongwei Ren, and Wangmeng Zuo. Unpaired learning of deep image denoising. In *European Conference on Computer Vision (ECCV)*, 2020. 3

- [29] L. P. Yaroslavsky. Digital picture processing - an introduction. *Springer Verlag*, 1985. 1
- [30] K. Zhang, W. Zuo, Y. Chen, D. Meng, and L. Zhang. Beyond a gaussian denoiser: Residual learning of deep cnn for image denoising. *IEEE Transactions on Image Processing*, 26(7):3142–3155, 2017. 3, 6